Low Phase Noise Array-Composite Micromechanical Wine-Glass Disk Oscillator

Yu-Wei Lin, Sheng-Shian Li, Zeying Ren, and Clark T.-C. Nguyen

Center for Wireless Integrated Micro Systems
Department of Electrical Engineering and Computer Science
University of Michigan, Ann Arbor, Michigan 48109-2122, USA
TEL: 734-764-5411, FAX: 734-647-1781, email: ywlin@umich.edu

ABSTRACT

A reduction in phase noise by 13 dB has been obtained over a previous 60-MHz surface-micromachined microme-chanical resonator oscillator by replacing the single resonator normally used in such oscillators with a mechanically-coupled array of them to effectively raise the power handling ability of the frequency selective tank. Specifically, a mechanically-coupled array of nine 60-MHz wine-glass disk resonators em-bedded in a positive feedback loop with a custom-designed, single-stage, zero-phase-shift sustaining amplifier achieves a phase noise of -123 dBc/Hz at 1 kHz offset and -136 dBc/Hz at far-from-carrier offsets. When divided down to 10 MHz, this effectively corresponds to -138 dBc/Hz at 1 kHz offset and -151 dBc/Hz at far from carrier offset, which represent 13 dB and 4 dB improvements over recently published work on surface-micromachined resonator oscillators, and also now beat stringent GSM phase noise requirements by 8 dB and 1 dB, respectively.

I. INTRODUCTION

Among off-chip components in a wireless communication circuit, the quartz crystal used in the reference oscillator is perhaps the most difficult to miniaturize, since Q's > 10,000 and thermal stabilities better than 35 ppm uncompensated over 0-70°C are generally unavailable on-chip. Recently, however, on-chip vibrating micromechanical resonators based on MEMS technology have become increasingly attractive as on-chip frequency selective elements for communication-grade oscillators and filters, spurred by demonstrations of Q's > 145,780 at 60 MHz [1], frequency temperature dependencies of only 18 ppm over 25-105°C at 10 MHz [2], and by a poten-tial for single-chip integration with transistors [3]. A recent reference oscillator using an SOI-based vibrating microme-chanical resonator [4] has, in fact, already satisfied the GSM specification (-130 dBc/Hz and -150 dBc/Hz at 1 kHz and far-from-carrier offsets, respectively, from a 13 MHz carrier). Oscillators employing *surface-micromachined* resonator tanks, however, encumbered by a smaller power handling ability, do not quite yet satisfy GSM specs [1] over all carrier offsets. Between SOI- and surface-micromachining, the latter is per-haps more attractive, since it avoids high-aspect ratios and has a more successful planar integration history [3][5].

Pursuant to attaining GSM reference oscillator phase noise specs using a *surface-micromachined* resonator tank, this work first recognizes that phase noise is inversely proportional to resonator tank power handling [6]; then proceeds to lower phase noise by coupling several micromechanical disk resona-tors into mechanical arrays that then automatically match up the individual resonator frequencies and combine their outputs to significantly raise the overall "composite" resonator power
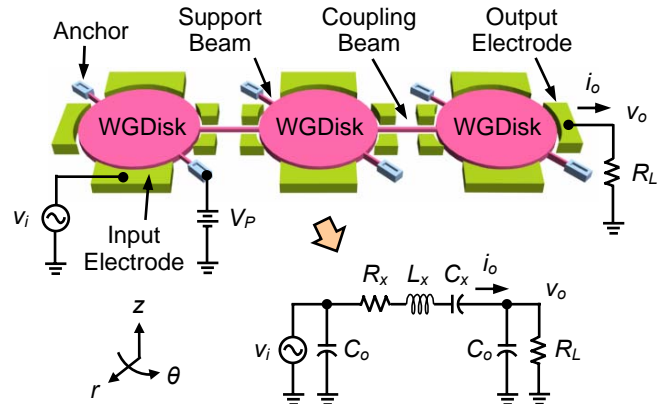

Fig. 1: Perspective-view schematic of a multi (three) wine-glass disk micro-mechanical resonator array. The electrical equivalent circuit for the resonator is shown to the bottom right.
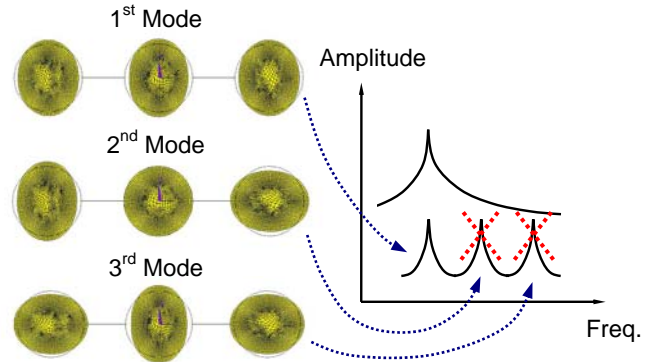

Fig. 2: ANSYS simulated mode shapes for a mechanically coupled three wine-glass disk micromechanical resonator array.

handling. This increase in power handling leads to oscillator phase noise improvements of up to 13 dB at close-to-carrier offsets, and yields an overall phase noise plot that handily sur-passes GSM specs. As will be shown, much of this rather large improvement actually derives from a removal of the $1/f^3$ close-to-carrier noise that before now had greatly limited the per-formance of micromechanical resonator oscillators.

II. WINE-GLASS DISK ARRAY RESONATOR

Fig. 1 presents the perspective-view schematic of a 3-resonator version of the wine-glass disk-array resonator used to raise power handling in this work, together with a typical two-port bias and excitation scheme, and an equivalent electri-cal model. Here, three (or more) wine-glass disks, each identi-cally designed to 60 MHz, are coupled mechanically by 1μm-wide, half-wavelength coupling beams connecting each adja-cent resonator to one another at high-velocity locations.
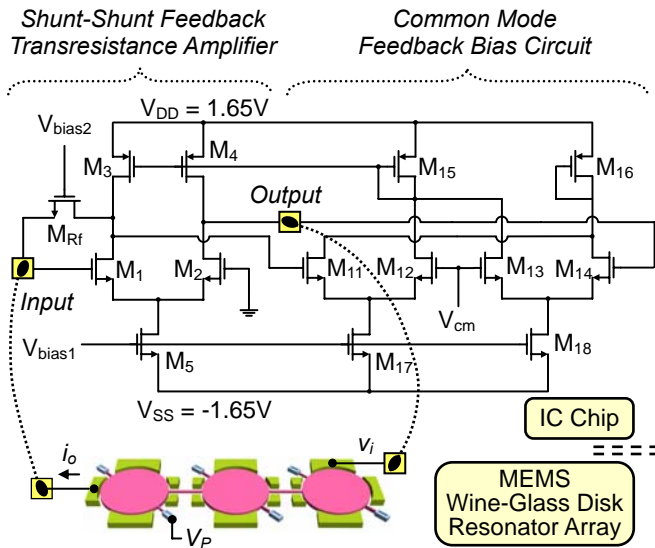
Fig. 3: Detailed circuit schematic of the single-stage sustaining transresistance amplifier of this work, implemented by a fully-differential amplifier in a one-sided shunt-shunt feedback configuration. Interconnections between the IC and MEMS chips were made via wire-bonding.

A. Constituent Wine-Glass Disk Resonators

As shown, each resonator in the array consists of a 32μm-radius, 3μm-thick, electrically conductive disk spaced 900 nm above the substrate, supported by two beams that attach to the disk at quasi-nodal points [1], where displacements are negligible compared to other parts of the disk structure when the disk vibrates in its wine-glass mode shape. In this mode shape, the disk expands along one axis and contracts in the orthogonal axis, as depicted in Fig. 2. Electrodes surround the disk with a lateral electrode-to-disk gap spacing of only 80 nm. To operate this device, a dc-bias V_P is applied to the disk structure, and an ac voltage v_i is applied to the input electrodes. (Note that there is no current flowing once the conductive structure is charged to V_P, so there is no dc power consumption). This $V_P v_i$ voltage combination generates a time-varying force proportional to the product $V_P v_i$ that drives the disk into the wine-glass mode shape when the frequency of v_i matches the wine-glass resonance frequency f_o, which is inversely proportional to the disk radius. ([1] provides a complete formulation for f_o.)

Once vibrating, the dc-biased (by V_P) time-varying output electrode-to-resonator capacitors generate output currents governed by the series motional resistance R_x of the resonator, given approximately by

$$R_x = \frac{v_i}{i_o} = \frac{k_r}{\omega_o Q V_P^2} \cdot \frac{d_o^4}{\varepsilon_o^2 A_o^2} \qquad (1)$$

where A_o and d_o are the electrode-to-resonator overlap area and gap spacing, respectively, of the wine-glass disk resonator; ε_o is the permittivity in the gap (in this case, of air); $\omega_o = 2\pi f_o$ is the radian resonance frequency; and k_r is the effective stiffness of the disk [1].

B. Resonator Array

As described in [7], the mechanical connection of resonators in Fig. 1 actually realizes a multi-pole filter structure that now has several modes of vibration. Each modal peak corresponds to a state where all resonators are vibrating at exactly
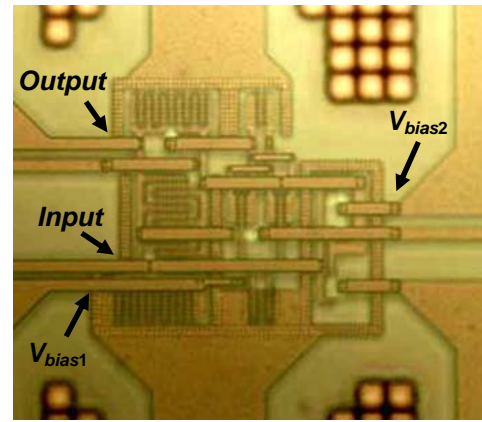

Fig. 4: Photo of the sustaining transresistance amplifier IC fabricated in TSMC's 0.35 μm CMOS process.

the same frequency. Fig. 2 presents ANSYS simulations showing the different modes of this structure, which are distinguishable by the phasings between the resonators. Because each mode exhibits unique resonator phasings, a single mode can be selected by choosing the input ac signal to match the phasing of the desired mode. In this work, the first mode of the array is selected. It should be noted that the use of half-wavelength coupling beams serves to spread the modal peaks of the filter structure in Fig. 1 far apart, which facilitates the selection of one, and only one, of the modes.

Once a single mode is selected, the structure practically behaves as a single resonator, but with a current handling ability equal to the sum of the currents from all constituent resonators. Thus, an *n-resonator* array can handle *n* times more power than a single resonator.

In the present oscillator application, the power handling limit of a micromechanical resonator is perhaps best specified by the power running through it when it vibrates at a maximum acceptable amplitude $X_{max} = ad_o$, where *a* is the fraction of the electrode-to-resonator gap d_o beyond which the onset of strong nonlinearities ensue. Using (6) from [8], the maximum power P_{omax} that a composite array resonator can handle can then be expressed by

$$P_{omax,n} = \frac{\omega_o}{Q_n} k_{rn} a^2 d_o^2 = n \cdot \frac{\omega_o}{Q_n} k_r a^2 d_o^2 \qquad (2)$$

where *n* is the number of resonators in the array; and k_{rn} and Q_n are the stiffness and quality factor of the array, respectively.

III. OSCILLATOR CIRCUIT DESIGN

To minimize *Q* loading of the composite array resonator, the transresistance CMOS sustaining amplifier used here (c.f., Fig. 3) is similar to that detailed in [1]. Briefly, this circuit differs from previous two-stage circuits in that it achieves the needed 0° phase shift for oscillation in only a single stage, which improves both its noise and bandwidth performance. Fig. 4 presents a photo of the amplifier IC, which was fabricated in TSMC's 0.35 μm CMOS process. The IC chip area is 50μm×50μm, which together with the $n×(105μm×105μm)$ required for the wine-glass disk array, yields a tiny combined footprint of less than 320μm×320μm for a 9-resonator array. Table 1 summarizes the design and performance of the overall oscillator circuit.

Table 1. Oscillator Data Summary

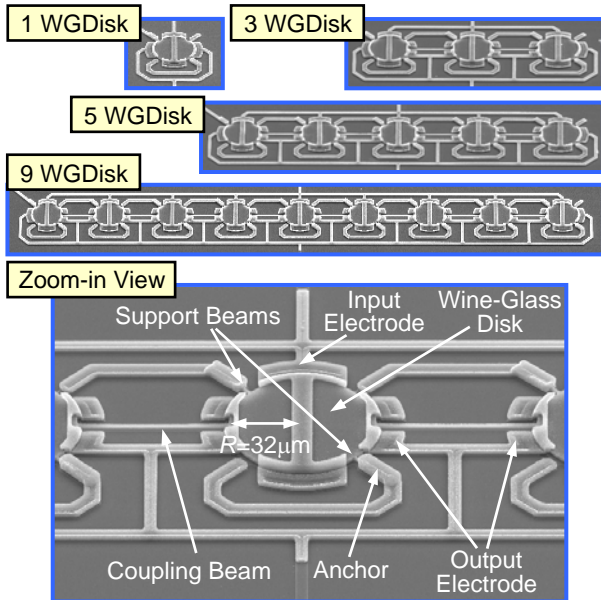| Oscillator Design Summary		
Integrated Circuit	Process	TSMC 0.35 μm CMOS
	Voltage Supply	± 1.65 V
	Power Cons.	350 μW
	Amplifier Gain	8 kΩ
	Amplifier BW	200 MHz
	Layout Area	50 μm × 50 μm
MEMS Wine-Glass Disk Resonator Array	Process	Polysilicon-Based Surface Micromachining
	Radius, R	32 μm
	Thickness, h	3 μm
	Gap, d_o	80 nm
	Voltage Supply	10 V
	Power Cons.	~ 0 W
	Motional Resistance, R_x	5.75 kΩ, 3.11 kΩ, 1.98 kΩ, 1.25 kΩ for n = 1, 3, 5, 9
	Layout Area	n × 105 μm × 105 μm

Fig. 5: SEM's of fabricated wine-glass disk resonator-arrays with varying numbers of mechanically-coupled wine-glass disks.

IV. EXPERIMENTAL RESULTS

Wine-glass disk array resonators were fabricated via a three-polysilicon self-aligned stem process used previously to achieve disk resonators [9]. Fig. 5 presents SEM's of fabricated 60-MHz wine-glass disk arrays with varying numbers of coupled resonators, each supported by only two support beams. Fig. 6 presents measured frequency spectra for a stand-alone wine-glass disk resonator together with resonator arrays using 3, 5, and 9 resonators mechanically coupled with one another. Although the single resonator achieves the highest Q of 161,000, the array Q's are still all greater than 115,000.

From the peak heights, R_x (with V_P = 7 V) can be extracted to be 11.73 kΩ, 6.34 kΩ, 4.04 kΩ, and 2.56 kΩ, for 1, 3, 5, and 9 resonator arrays, respectively. The measured R_x reduction factors of 1.85, 2.90, and 4.58, actually fall short of the expected 3, 5, and 9, respectively (i.e., the number of the reso-
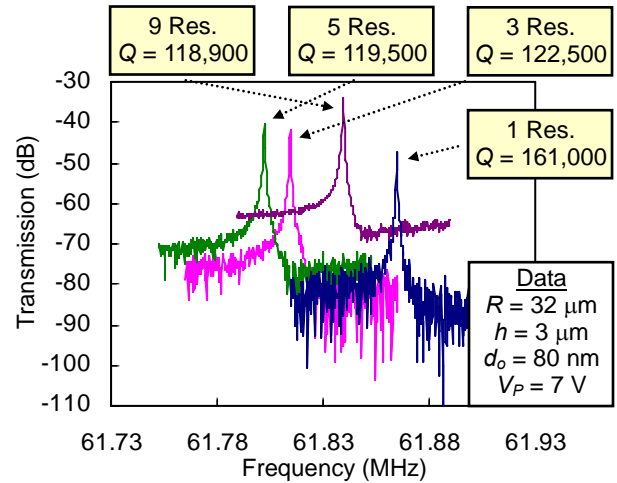

Fig. 6: Measured frequency characteristic for a fabricated wine-glass disk resonator-array.
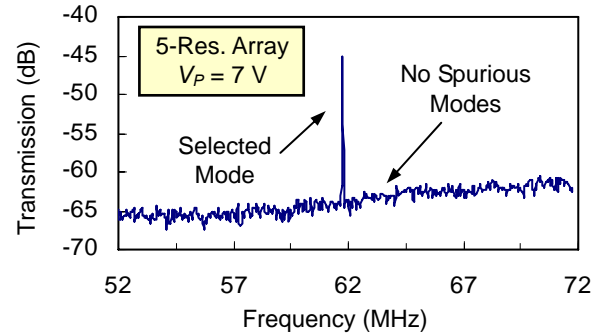

Fig. 7: Measured frequency spectrum verifying no spurious modes around the desired mode of the resonator array, achieved via proper electrode excitation and half-wavelength coupling beam design.

nators in the array). Although differences in Q contribute somewhat to the lower multiplication factor, the main culprit here is the need to split the electrodes between resonators in order to avoid coupling beams located at high velocity points (c.f., Fig. 1). Since the coupling beams attach at high velocity points, the electrodes between resonators must be split and removed at high velocity points where the current would otherwise have been the largest. This greatly reduces the current contribution from such inner electrodes, thereby reducing the factor by which the motional resistance is lowered. A more detailed determination of R_x using velocity integration over each electrode (e.g., as done in [10]) yields reduction ratios of 1.84, 2.85, and 4.94, for the 3, 5, and 9 resonator arrays, respectively, which now match the measured values.

Note that the square resonators of [7] did not suffer from the above problem, since their coupling beams did not interfere with their electrodes. One remedy to the problem for disk resonators is to couple the disks in a third plane above them, which would keep the coupling beams clear of the electrodes, but at the penalty of another masking step.

To ascertain how effectively unwanted modes in the mechanically coupled array have been suppressed, Fig. 7 presents the frequency characteristic for a 5-disk array measured over a wide frequency range (20 MHz). Here, only a single peak corresponding to the first filter mode is observed, which verifies the utility of half-wavelength coupling beam design and electrode placement in eliminating unwanted modes.
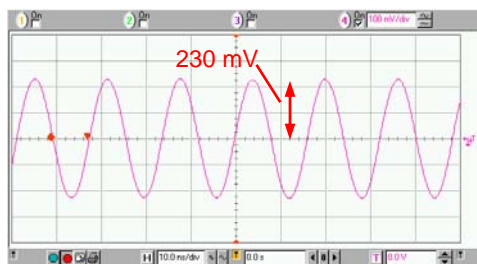
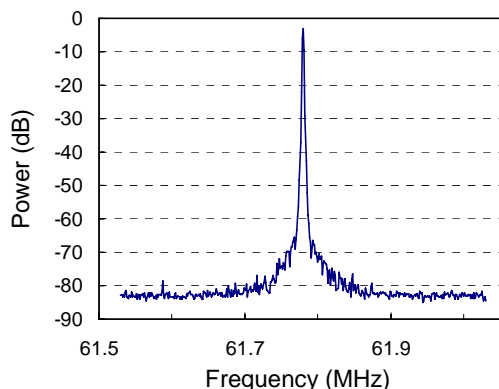Fig. 8: Measured steady-state oscilloscope waveform for the 60-MHz wine-glass disk resonator-array oscillator.

Fig. 9: Measured steady-state Fourier spectrum for the 60-MHz wine-glass disk resonator-array oscillator.
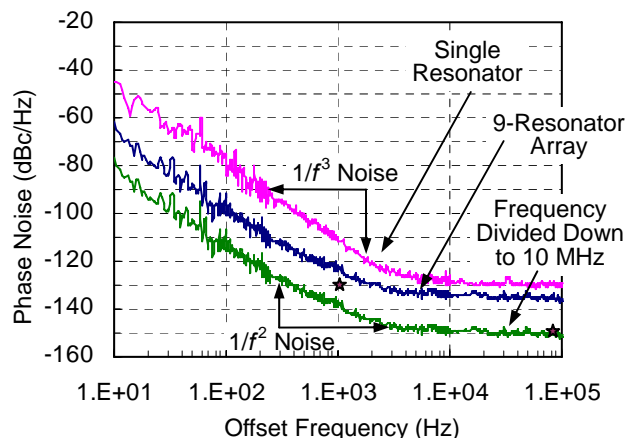

Fig. 10: Phase noise density versus carrier offset frequency plots for the 60-MHz wine-glass disk resonator-array oscillator, measured using an HP E5500 Phase Noise Measurement System. The two star symbols show the GSM specification for close-to-carrier and far-from-carrier offsets.

For oscillator testing, the IC and MEMS chips were interconnected via wire-bonding, and testing was done under vacuum to preserve the high Q of the micromechanical resonators or arrays. Figs. 8-10 present oscillator performance data, starting with the obligatory oscilloscope and spectrum analyzer waveforms, and culminating in a plot of phase noise density versus offset from the carrier frequency. The last of these shows a phase noise of -123 dBc/Hz at 1 kHz offset from the carrier, and -136 dBc/Hz at far-from-carrier offsets. This far-from-carrier noise floor is about 4 dB better than that of an oscillator using a single wine-glass disk resonator, verifying the utility of resonator array design. In addition, Fig. 10 also shows that the undesired $1/f^3$ noise (seen in previous micromechanical resonator oscillators [1]) is removed when a coupled array is utilized, due to its increased power handling ability. With $1/f^3$ noise suppressed, an expected $1/f^2$ dependence commonly exhibited by high Q oscillators then remains, improving the close-to-carrier phase noise at 1 kHz offset from -110 dBc/Hz to -123 dBc/Hz. Dividing down to 10 MHz for fair comparison, this corresponds to -138 dBc/Hz at 1 kHz offset and -151 dBc/Hz far from the carrier, which more than satisfies (by 8 dB and 1dB) the stringent GSM requirement.

V. CONCLUSIONS

Via use of a mechanically-coupled array approach to boost the power handling ability of a "composite" micromechanical resonator, a 60-MHz series resonant oscillator divided down to 10 MHz has been demonstrated with phase noise values of -138 dBc/Hz at 1 kHz offset and -151 dBc/Hz at far-from-carrier offsets, both of which now satisfy stringent GSM specifications for communications reference oscillators. This, together with its low power consumption of only 350 μW, and its potential for full integration of the transistor sustaining circuit and MEMS device onto a single silicon chip, makes the micromechanical resonator-array oscillator of this work an attractive on-chip replacement for quartz crystal reference oscillators in communications applications. And all of this made possible by effectively harnessing the integration advantage of micromechanics, which allows a designer to break the "minimalist" paradigm that dictates the use of one and only one quartz crystal in an oscillator, and instead, permits the use of as many micromechanical resonators as needed, with little size or cost penalty.

REFERENCES

[1] Y.-W. Lin, S. Lee, S.-S. Li, Y. Xie, Z. Ren, and C. T.-C. Nguyen, "Series-resonant VHF micromechanical resonator reference oscillators," *IEEE J. Solid-State Circuits*, vol. 39, no. 12, pp. 2477-2491, Dec. 2004.

[2] W.-T. Hsu and C. T.-C. Nguyen, "Stiffness-compensated temperature-insensitive micromechanical resonators," *Technical Digest*, MEMS'02, Las Vegas, NV, 2002, pp. 731-734.

[3] A. E. Franke, J. M. Heck, T.-J. King, and R. T. Howe, "Polycrystalline silicon-germanium films for integrated microsystems," *J. Microelectro-mechanical Systems*, vol. 12, no. 2, pp. 160-171, April 2003.

[4] V. Kaajakari, T. Mattila, A. Oja, J. Kiihamäki, and H. Seppä, "Square-extensional mode single-crystal silicon micromechanical resonator for low-phase-noise oscillator applications," *IEEE Electron Device Letters*, vol. 25, no. 4, pp. 173-175, April 2004.

[5] T. A. Core, W. K. Tsang, S. J. Sherman, "Fabrication technology for an integrated surface-micromachined sensor," *Solid State Technology*, vol. 36, no. 10, pp. 39-47, Oct. 1993.

[6] W. P. Robins, *Phase Noise in Signal Sources.* London: Peter Peregrinus, Ltd., 1982.

[7] M. U. Demirci, M. A. Abdelmoneum, and C. T.-C. Nguyen, "Mechanically corner-coupled square microresonator array for reduced series motional resistance," *Digest of Technical Papers*, Transducers'03, Boston, MA, 2003, pp. 955-958.

[8] S. Lee and C. T.-C. Nguyen, "Mechanically-coupled micromechanical resonator arrays for improved phase noise," *Proceedings*, IEEE Int. Ultrasonics, Ferroelectrics, and Frequency Control 50th Anniv. Joint Conf, Montreal, Canada, Aug. 2004, pp. 280-286.

[9] J. Wang, Z. Ren, and C. T.-C. Nguyen, "1.156-GHz self-aligned vibrating micromechanical disk resonator," *IEEE Trans. Ultrason., Ferroelect., Freq. Contr.*, vol. 51, no. 12, pp. 1607-1628, Dec. 2004.

[10] F. D. Bannon III, J. R. Clark, and C. T.-C. Nguyen, "High-Q HF microelectromechanical filters," *IEEE J. Solid-State Circuits*, vol. 35, no. 4, pp. 512-526, April 2000.